Content Appeared in the May / June 2003 IEEE Industry Applications (Vol. 9, No. 3 · ISSN 1077-2618)

# HEV S/G

High-effciency operation of a HYBRID ELECTRIC VEHICLE STARTER/GENERATOR over road profiles.

BY RAYMOND B. SEPE, JR., CHRIS MORRISON JOHN M. MILLER, & ALLAN R. GALE

EFFICIENT OPERATION OF INDUCTION motor starter/alternator systems is an important part of the power-management function that is required in the self-con-tained vehicular environment. However, the nonlinear dynamics of the induction motor [1], parameter sensitivity to environmental factors, load complexities, and vehicular performance requirements make it difficult to determine and sustain the most efficient operating points. This article characterizes the performance of a fuzzy-logic controller for a hybrid electric vehicle (HEV) starter/generator (S/G) that is used to maintain optimum efficiency operation under both steady state and dynamic loading conditions. In steady-state conditions, automatic mapping of the maximum-efficiency operating points is achieved. Based on this data, the maximum possible efficiency under dynamic load profiling can be determined. In-vehicle dynamic loading is then emulated in the laboratory using a motor-development platform that can replay industry standard FTP75 road profiles and apply them to the S/G. The effects of velocity transients and the bandwidth of the fuzzy controller on efficiency are presented. The effectiveness of the fuzzy controller in maintaining high-efficiency operation and in reduced heating is demonstrated.

The induction machine S/G and HEV architecture is described in [2]. For this work, the 8-k W, 12-pole machine windings were parallel connected in alternator configuration. The efficiency data in [2] was derived by careful manual measurement techniques with close monitoring of machine temperature. The objective here was twofold. First, to automate the mapping of steady-state optimum efficiency points using a real-time system. Second, to be able to sustain maximum-efficiency operation over road-loading conditions. In both cases, minimal sensitivity to environmental changes is also required. Vehicular deployment of such a system could be used to automatically maintain maximum S/G efficiency in the HEV.

**A FUZZY-LOGIC CONTROLLER EFFECTIVELY AUTOMATICALLY OPERATES AN HEV S/G AT ITS MAXIMUM EFFICIENCY.**

Because of the complexities and variability involved in modeling and controlling induction motor systems for automotive applications, recent work has focused on fuzzy-logic control techniques [3], [4]. In [3], fuzzy logic is used for automobile engine control, but energy efficiency is not addressed. The architecture of the fuzzy controller used here is based on [4]. This work is a continuation of [5]. It extends the results presented there to include dynamic ef-ficiency optimization over the industry standard FTP 75 road profile. It addresses transient behavior and controller bandwidth as related to efficiency over realistic dynamic loading conditions not found in previous work.

## Fuzzy-Logic Controller

### *Architecture*

Induction machines are normally operated at rated flux to achieve their best dynamic response [6]. However, under less-than-rated load conditions, operation at rated flux can cause excessive core losses that result in below-optimum efficiency. Under these conditions, the flux can be reduced with the objective of achieving optimum-efficiency operation. The fuzzy-logic controller is used to automatically determine the proper flux level for optimum-efficiency operation under varying load and temperature. However, the reduction of flux also decreases the transient response of the motor. The tradeoff between dynamic response and efficiency is application dependent. Here the objective is maximum-efficiency operation.

Figure 1 is a block diagram of the system control structure, where $I_d$ is direct axis current, $I_q$ is quadrature axis current, and * is a commanded quantity. An inner-loop, indirect field-oriented vector-current controller is used to regulate the motor currents. This allows control of rotor flux in proportion to $I_d$*, and electromagnetic torque in proportion to the product of $I_d$* and $I_q$* [6]. A mechanical observer with input from a 4,096-count shaft encoder is used to generate rotor position and speed estimates. The velocity controller generates $I_q$* for the current controller based on the required torque and the value of $I_d$*. Because the velocity con-trol-ler tries to maintain a constant torque under steady-state operation, any changes in $I_d$* cause torque perturbations that are automatically negated by the velocity controller via an updated $I_q$*.

The fuzzy logic efficiency-optimizing controller adjusts the motor's flux using $I_d$*. Its objective is to maximize the S/G electrical-output power for constant mechanical-input power. It accomplishes this by perturbing $I_d$* and reacting to the resulting change in electrical-output power. If the

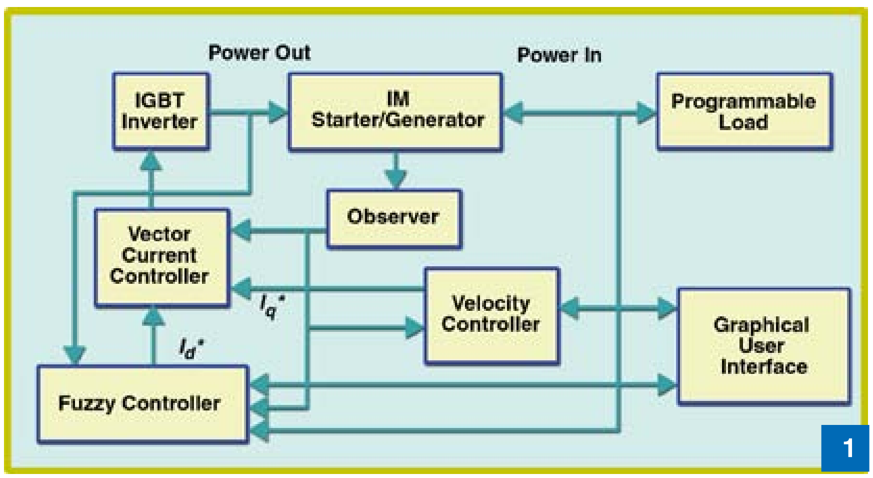


**Control system block diagram.**

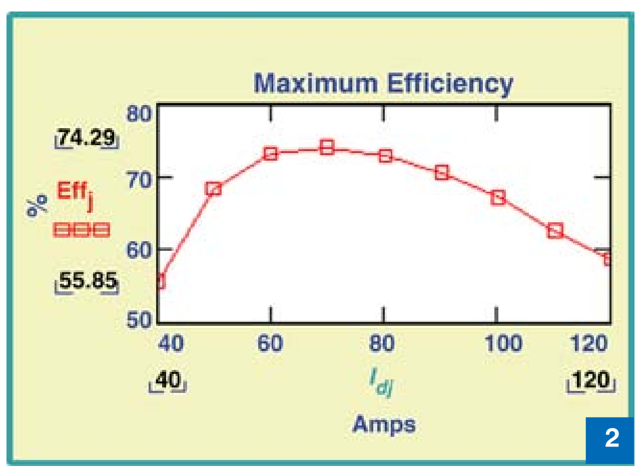


**Measured S/G efficiency as a function of $I_d$.**

power output increases, it continues to perturb $I_d$* in the same direction. The fuzzy-logic controller uses 14 fuzzy-logic rules and triangular membership functions in determining its output command. A more detailed description of the fuzzy algorithm can be found in [5]. Note that the power-in signal in Figure 1 is used to calculate system efficiency for diagnostic purposes but is not needed by the fuzzy-control algorithm.

Figure 2 is a plot of the motor ef-ficiency as a function of $I_d$. It graph-ically shows the objective of the fuzzy controller.

At constant 20kW operating point, notice that the efficiency curve is a bell shape with a maximum point of about 75% at $I_d$ = 70 A. The fuzzy controller must tune $I_d$ to reach this maximum and continue to track subsequent maximum-efficiency points as they change with time and operating conditions.

## Steady-State *Efficiency Mapping*

The fuzzy controller has been used to automatically find the maximum-efficiency operation that can be achieved at each user-specified torque-speed set point. The user enters ten arbitrary torque-speed operating points into a fuzzy-system mapping table. The fuzzy controller then adjusts $I_d$ until the S/G is operating at maximum efficiency. The efficiency data is then automatically entered into the right-hand column of the mapping table before the system proceeds to the next tabulated set point.

Figure 3 shows the experimental results of maximum-efficiency mapping across constant power contours of 1, 2, 4, 6, and 8 kW.

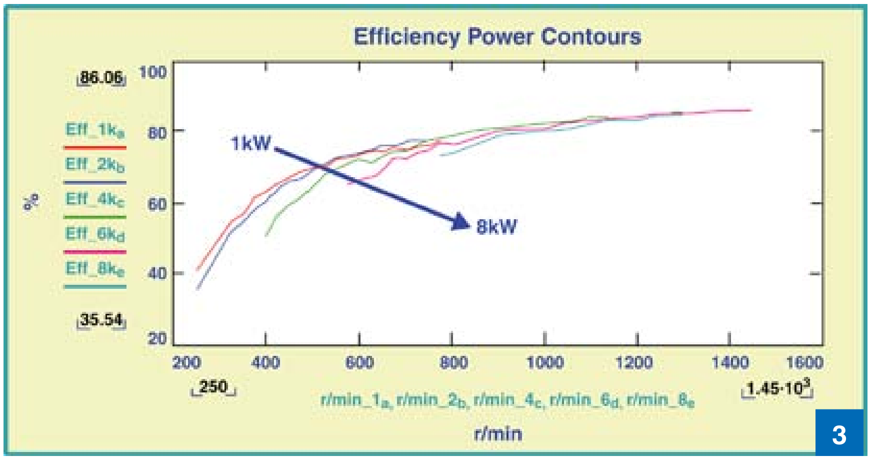


S/G efficiency for 1-. 2-, 4-, 6-, and 8-kW steady-state constant power contours.

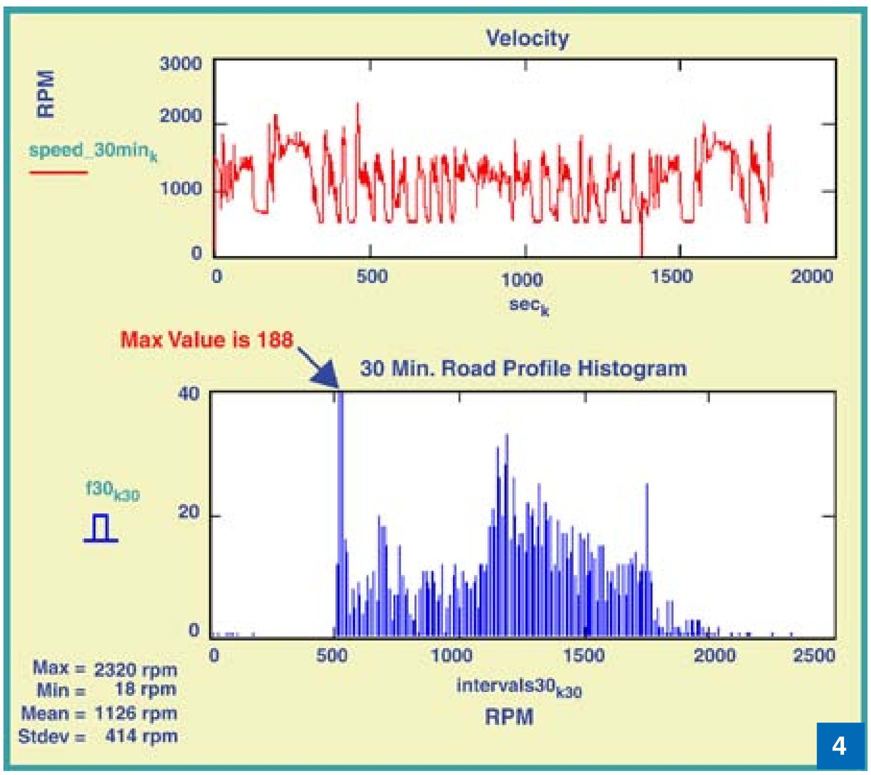


FTP75 30-min drive cycle.

| Table 1. Baseline Maximum-Efficiency Performance. | |
|---|---|
| Mean | 79.4% |
| Maximum | 83.9% |
| Minimum | 20.2% |
| Standard Deviation | 6.2% |

Notice that S/G efficiency is about 85 % at 1,400 r/min but is as low as 35% at speeds below 300 r/min. An efficiency-optimization algorithm that locates the S/G maximum-efficiency operating points for a given torque and speed can be found in [5]. This allows prediction of performance based on S/G parameters and can be used as a design tool. Note that the effect of saturation must be included to accurately predict performance at lower speeds.

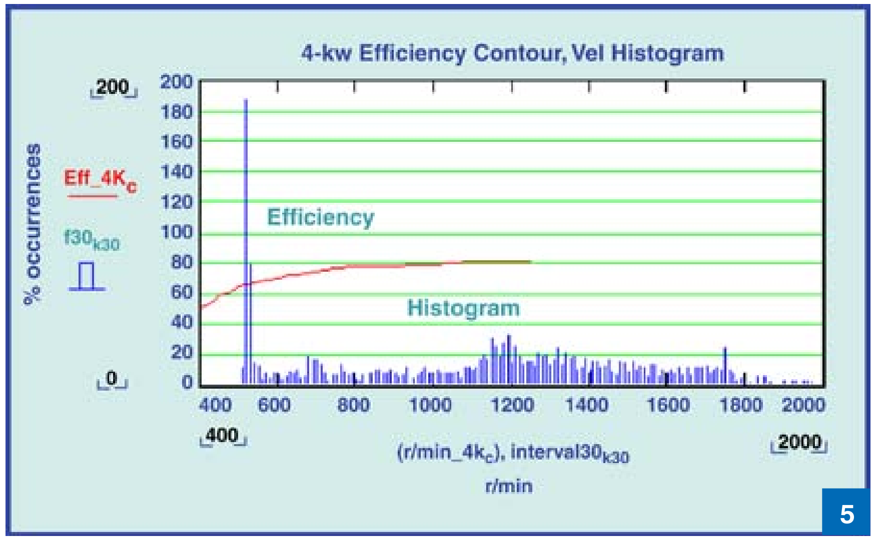


Efficiency for 4-kW contour and histogram.

## Drive-Cycle Data

A statistical analysis was performed on the FTP75 drive cycle. Figure 4 contains the engine velocity in revolutions per minute over the entire 30-min profile in the upper plot and statistics on the profile and a histogram of the data in the lower plot. The period between velocity data points is 1s. Histogram bins are 10-r/min wide.

It can be seen that the average velocity is 1,126 r/min. The histogram shows that there are two frequent re-gions of engine velocity: one between 500-800 r/min and the other between 1,100-1,800 r/min.

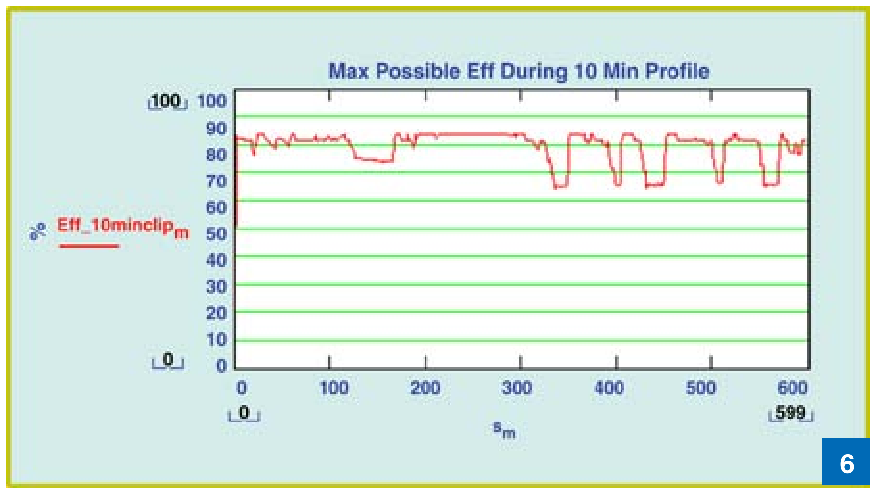


Maximum achievable efficiency at 4-kW output.

Figure 5 pots the efficiency over a 4-kW power contour on the same graph as the velocity histogram for the 30-min drive cycle. It can be seen that there is significant operation in the low-speed region where the efficiency is below 80%. This is also evident from the statistical data in Figure 4, which shows the mean operation a 1,126 r/min with a standard deviation of 414 r/min. This indicates that the low end of the velocity spread about the means is at 712 r/min. The efficiency plot indicates operation below 80% at that point. If this drive cycle is highly likely, this may imply a design goal of higher efficiencies at lower speeds for the S/G.

To determine the maximum achievable efficiency over the drive cycle with this S/G, the measured maximum-efficiency data from the steady-state efficiency mapping can be applied in simulation to each point in the drive cycle. This analysis yields a baseline for the best performance that can be achieved by the fuzzy controller if it had no bandwidth limitations. Because the measured efficiency data points do not necessarily coincide with each drive-cycle ve-locity point, a polynomial curve fit is used to generate a formula for efficiency as a continuous function of velocity.

In order to facilitate algorithm development testing, the first 10 min of the drive cycle were used, and the maximum velocity was limited to 1,550 r/min to reflect hardware limitations in the experimental test bed. Table 1

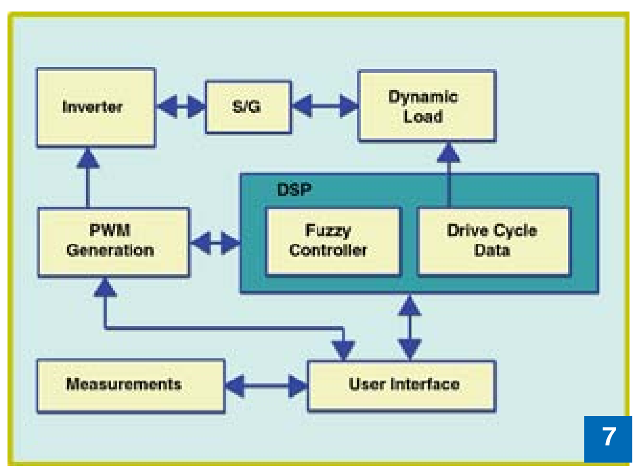


Block diagram of experimental system.

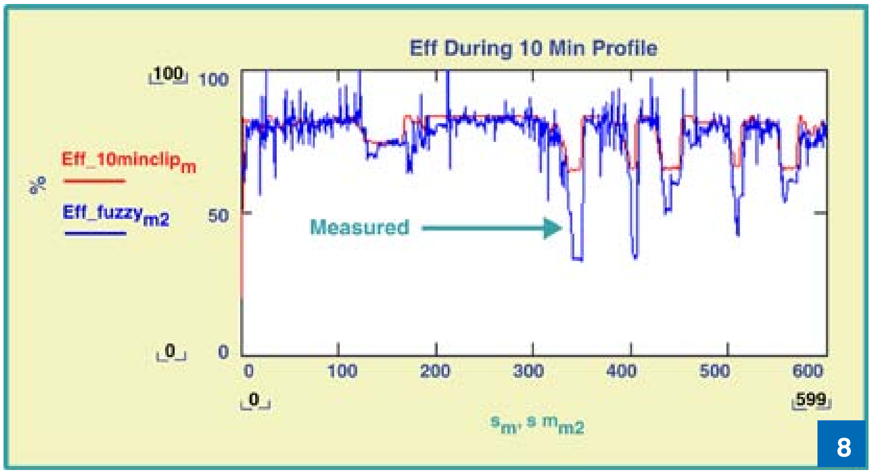

**Comparison of best achievable efficiency and measured fuzzy efficiency.**

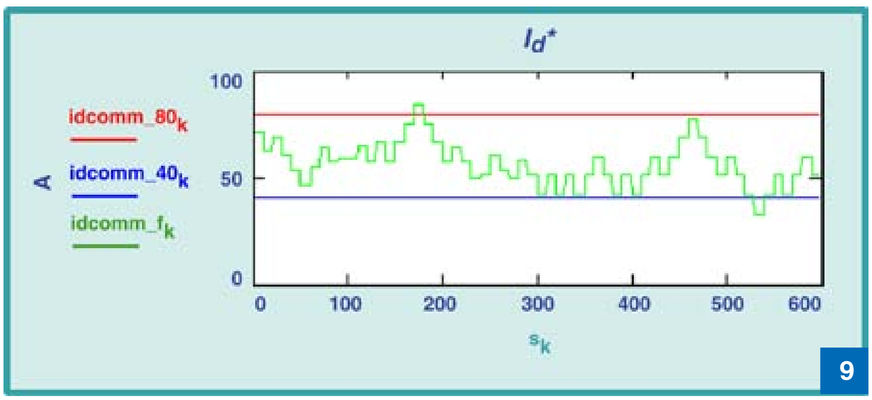

**Fuzzy controller continuously tuning *Id* during road profile.**

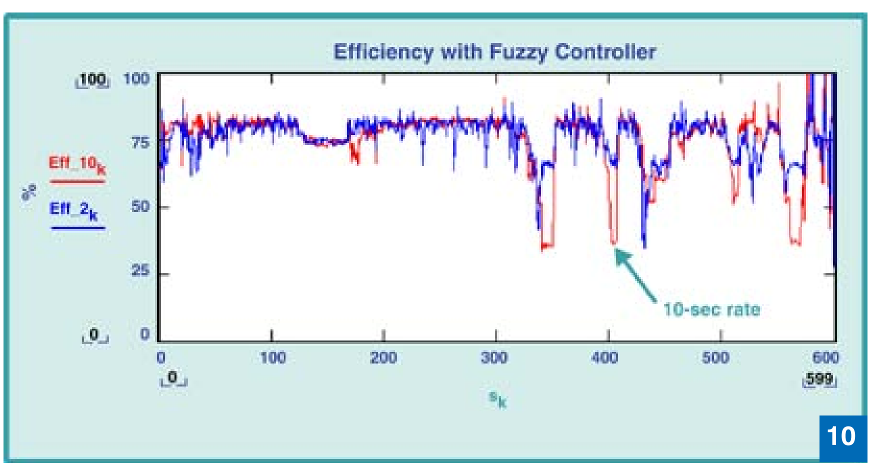

**Efficiency with 10- and 2-s fuzzy controller update rates.**

contains the statistical summary, and Figure 6 plots the maximum achievable efficiency. This is the baseline for measured performance in subsequent sections.

## Experimental Setup

Figure 7 is a block diagram of the system architecture used to apply drive-cycle data to the S/G. The drive-cycle data file is stored on the PC and then via the user interface. The selected drive-cycle data is automatically downloaded onto the digital signal processor (DSP) as part of the code initialization. The DSP then issues commands to the programmable-load motor system in real-time by reading the drive-cycle data directly from its memory.

The dynamic load system is operated under speed control. The S/G is operated in constant power mode. In constant power mode, the desired shaft power is divided by the estimated motor speed to generate a shaft torque command. Af-ter adding the effects of friction, an electromagnetic torque command is developed. The current $I_q$* is then automatically adjusted to maintain the commanded electromagnetic torque as the fuzzy controller works to tune $I_d$*. This is, effectively, a feed-forward controller that works to regulate the mechanical power at the shaft. Therefore, constant power experiments performed here refer to constant power at the shaft.

## Fuzzy Optimization over Road Profile

A drive-cycle fuzzy-power optimization experiment was conducted at a shaft power of —4kw over the 10-min road profile. The fuzzy optimizer takes a new fuzzy step every 10 s. Figure 8 shows the system efficiency using the fuzzy optimizer superimposed on the maximum achievable system efficiency previously shown in Figure 6. The noisy spikes are due to transients. It can be seen that the fuzzy system follows the contour of the best achievable efficiency profile but with some difficulty in transient areas of operation.

In examining the operation of the system during this experiment, it was found that the fuzzy controller automatically moves $I_d$ between 80 and 40 A, as required during the profile (Figure 9). In particular, in the 150-175s region, best performance is achieved for $I_d$ = 80 A while $I_d$ = 40 A is best in the region between 175-325 s. In spite of its ability to automatically move $I_d$, a constant $I_d$ command during a transient period in the road profile sometimes outperforms the fuzzy controller. This implies that the limited bandwidth of the fuzzy controller can adversely affect performance during transients.

An experiment was conducted to operate the fuzzy controller at different update rates to determine the effect of bandwidth over the road profile. Two experiments were conducted in which the fuzzy controller update rate was set to 10 and 2 s, respectively. Figure 10 compares the performance of the fuzzy controllers. The 2-s update rate yields improved transient tracking and, therefore, gives a higher efficiency over the road profile.

For points of comparison, 4-kW constant power experiments were performed with $I_d$* fixed at 80 A, with $I_d$* fixed at 40 A, and with $I_d$* adjusted by the fuzzy optimizer, with a 10- and 2-s update rate. The relative efficiency is evident in the measured stator temperature of the S/G during the road profile. Examining Figure 10 notice that the stator temperature is lowest using the fuzzy controller with a 2-s update rate. Notice, too, that the fuzzy controller with the 10-s update rate results in a higher transient temperature and a similar final temperature as using a fixed $I_d$ at 40 A (Figure 11).

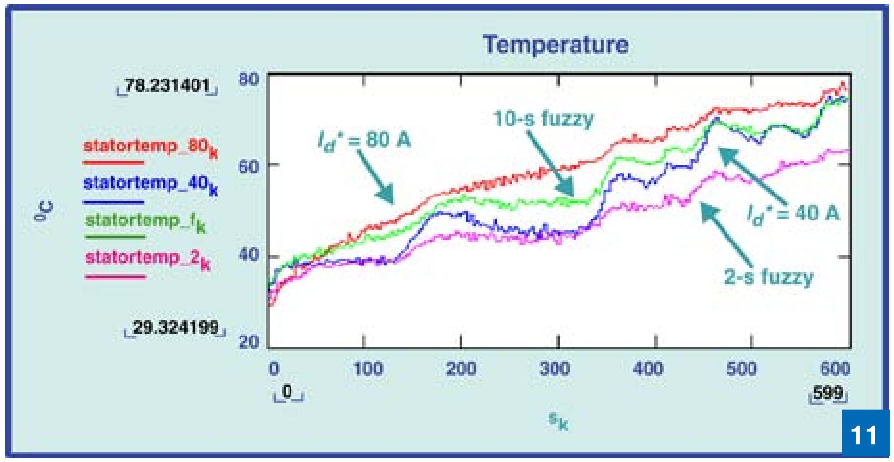


**Stator temperature over road profile with $I_d$ fixed at 80 and 40 A, fuzzy controller with 10-s update rate, and fuzzy controller with 2-s update rate.**

## Summary


This article demonstrates the effectiveness of a fuzzy-logic controller to automatically operate an HEV S/G at its maximum efficiency under static conditions and over industry-standard road-profile dynamic loads. The effects of transient behavior and controller bandwidth are investigated. Experimental results also show that reduced heating can be achieved.


## References


[1] B.K. Bose, *Power Electronics and Variable Frequency Drives*, Piscataway, NJ: IEEE Press, 1997.

[2] J.M. Miller, A.R. Gale, P.J. Mc Cleer, F. Leonardi, and J.H. Lang, “Starter-alternator for hybird electric vehicle: Comparison of induction and variable reluctance machines and drives,” in *Proc. IEEE IAS Annu. Meeting*, 1998, pp 513-523.

[3] J.M. Dongmo, F.M Salam, and G. Erten, “Adaptive fuzzy control of ac motors for electric vehicles and manufacturing systems,” in *Proc. 1996 IEEE Int. Symp. on Intelligent Control*, 1996, pp 408-413.

[4] G. Sousa, B.K. Bose, and J. Cleland, “Fuzzy logic based on-line efficiency optimization control indirect vector controlled induction motor drive,” in *IEEE-IECON Conf. Rec.*, 1993 pp. 1168-1174.

[5] R.B. Sepe JR., J.M. Miller, and A.R. Gale, “Intelligent efficiency mapping of a hybrid electric vehicle starter/alternator using fuzzy logic,” in *Proc. IEEE 18th Digital Avionics System Conf.*, 1999, vol. 2, pp. 8.B.2-1-8. B.2-8.

[6] D.W. Novotny and T.A. Lipo, *Vector Control and Dynamics of AC Drives*, London, UK: Clarendon Press, 1996.



*Raymond B. Sepe, Jr., (rsepe@electrostandards.com) and Chris M. Morrison are with Electro Standards Laboratories in Cranston, Rhode Island, USA. John M. Miller and Allan R. Gale are with Ford Motor Company in Dearborn, Michigan, USA. This article first appeard in its original form at the 2001 IEEE IAS Anuual Meeting.*